The Supernova SN2011dh: A new member of the rare SN IIb-subtype family

D. Dimitrov[1], D. Kjurkchieva[2]
[1] Institute of Astronomy and NAO, Bulgarian Academy of Sciences
[2] Department of astronomy, Shumen University
dinko@astro.bas.bg;d.kyurkchieva@shu-bg.net
(Submitted on 05.05.2013; Accepted on 15.06.2013)

Abstract. We present *BVRI* photometric observations and low-resolution spectra of the Supernova SN2011dh in M51 galaxy obtained at the NAO Rozhen. Its light curve was classified as SN II-L type with a peak absolute magnitude of $M_{\rm V} = -17.18^m$. The most prominent HeI 5876 feature of the spectra at the beginning of August 2011 was considerably (4 – 5 times) deeper and broader than the Hα line while they were almost the same a month earlier. The expansion velocities of all spectral features in August were smaller by 1550 – 2950 km/s than those a month earlier. The mean difference between the expansion velocities of Hα and HeI 5876 in August was around 3640 km/s. The disappearing of the Hα line and the strengthening of the HeI features visible on the NAO Rozhen spectra provided additional, sure confirmations that the Supernova SN2011dh is a new member of the rare SN IIb family.
Key words: galaxies: individual (NGC 5194) – stars: evolution – supernovae: general – supernovae: individual (SN 2011dh)

Introduction

All types of Supernovae (SNe) are important for modern astrophysics due to their role in our understanding of the stellar evolution and galactic nucleosynthesis.

Supernovae are classified according to the absorption lines that appear in their spectra. If a SN spectrum contains a line of hydrogen it is classified type II; otherwise it is type I.

The second important difference between the two main SN types is that the peaks of absolute magnitudes of type II Supernovae are dimmer than those of type I. Moreover, they vary considerably from one to another, while those of SN I are almost equal.

The third difference between the two main SN types is the average decay rate of the light curves: that of SN II is much lower than that of type I Supernovae.

It is widely assumed that a type II Supernova results from the rapid collapse and violent explosion of a massive star (9 – 50 $M_{\odot}$).

The SN II stars are sub-divided into two classes, depending on the shape of their light curves. The light curve for a type II-L supernova shows a steady (linear) decline following the peak brightness. The light curve of a type II-P supernova has a distinctive flat stretch (plateau) during the decline. The light curves of type II-L supernovae are explained by the expulsion of most of the hydrogen envelope of the progenitor star while the plateau phase in type II-P supernovae is attributed to the change in the opacity of the exterior layer due to ionization of the hydrogen in the outer envelope by the shock wave. This prevents photons from the inner parts of the explosion from escaping until the hydrogen cools sufficiently to recombine and the outer layer becomes transparent.

Additionally, Ensman & Woosley (1987) introduced IIb class which early-time spectra show prominent, high-velocity H lines, decreasing with time and disappearing completely about two months after the explosion. In the same period He I lines become the most prominent spectral features, i.e. in the late nebular phases their spectra more closely resembles a type Ib supernova. It was assumed that such a hybrid spectroscopic behavior of SNe, combining spectral features of both type II and type Ib spectra is a result of the explosion of a He core of an originally massive star, which had retained a residual (though marginal) H envelope at the time of explosion. As the ejecta of a type IIb expands, the hydrogen layer quickly becomes more transparent and reveals the deeper layers.

A progenitor star for type IIb SNe has been suggested to be a massive star which has lost most of its hydrogen envelope during its evolution, either by a strong wind or by a transfer to a binary companion (Filippenko et al. 1993; Filippenko 1997; Nomoto et al. 1993; Woosley et al. 1994).

The sizes of the hydrogen envelopes of SNe IIb are suggested to be diverse (Chevalier & Soderberg 2010), spanning from the "extended" progenitors of the red supergiant dimension surrounded by a dense wind ("eIIb" subclass) to the "compact" progenitors of the Wolf-Rayet star with a lower density, probably fast, wind ("cIIb" subclass). The H envelope mass dividing these categories is $\sim 0.1 M_{\odot}$. Compact progenitors give rise to fast shock waves and modulated radio light curves of SN cIIb while extended progenitors are characterized by slower shock waves and smoother radio curves of SN eIIb.

The goal of our *BVRI* photometric and low-dispersion spectral observations of SN2011dh was to provide additional empirical data about its subclassification.

1. The target SN2011dh

SN2011dh was discovered in images taken on May 31.893 (UT) by A. Riou (2011) in France. Several hours later, the Palomar Transient Factory (PTF, Law et al. 2011) collaboration detected the Supernova in images taken by the Palomar 48-inch Oschin Schmidt Telescope (P48) at a magnitude of $m_{\rm g}$=13.15 (Arcavi et al. 2011a).

PTF11eon/SN2011dh exploded in M51 (NGC 5194), a very nearby interacting spiral galaxy Whirlpool. The SN position is offset 126″ East and 91″ Sought from the nucleus of M51, along a prominent spiral arm.

The *UBVRI* photometry of Tsvetkov et al. (2012) exhibited that the light curves of SN2011dh are similar to those of SNIIb 2008ax but the initial flash is stronger and shorter, and there are humps in U and B on the onset of the linear decline.

The confirmation spectrum by Silverman et al. (2011) showed a relatively blue continuum and well-developed P-Cygni profiles in the Balmer lines with the Hα absorption minimum blueshifted by 17600 km/s. Arcavi et al. (2011b) classified SN2011dh as type II. They suspected its SN IIb nature before sure identifying of He features.

The target was detected early with the X-ray telescopes on *Swift* and on *Chandra* (Margutti & Soderberg 2011, Soderberg et al. 2012), ultraviolet-optical telescope on *Swift* (Kasliwal & Ofek 2011), Combined Array for Research in Millimeter-wave Astronomy (Horesh et al. 2011a) and Expanded Very Large Array (Horesh et al. 2011b). Marti-Vidal et al. (2011) reported on the VLBI detection of SN2011dh at 22 GHz which observations took place 14 days after the discovery of the Supernova, thus resulting in a VLBI image of the youngest radio-loud Supernova ever. This image revealed a very compact source.

Using pre-explosion images from the HST archive Maund et al. (2011) and Van Dyk et al. (2011) derived that the pre-SN source is a yellow supergiant (YSG) star with a radius $R \approx 270 R_{\odot}$ and without any clear evidence of a companion star contributing to the observed energy distribution.

At present there is a controversy in the literature about the actual progenitor size of SN 2011dh. On one hand, some authors suggested that the exploding star should be compact (Arcavi et al. 2011b, Soderberg et al. 2012, Szczygie et al. 2012) based on: the comparison between the early light curve of SN 2011dh and SN 1993J; the discrepancy between the temperature derived from an early-time spectrum and that predicted for an extended progenitor; the large shock velocity derived from radio observations.

On the other hand, the hydrodynamical modelling (Bersten et al. 2012, Benvenuto et al. 2012) indicates that the observations of SN 2011dh are compatible with a helium star progenitor of a mass near $4M_{\odot}$ surrounded by a thin hydrogen-rich envelope ($\approx 0.1M_{\odot}$) with a radius of $\sim 200R_{\odot}$. Such large radius is needed to reproduce the early light curve of SN 2011dh without contradicting the temperatures derived from the spectra.

Moreover, there were considerations suggesting that the progenitor of SN 2011dh should be a component of a binary system. However, a recent work by Georgy (2012) proposed that single YSG stars are plausible progenitors of SN 2011dh. Its latest images (Ergon et al. 2013, Van Dyk 2013) confirm this conclusion.

2. Observations at NAO Rozhen

We carried out observations of SN 2011dh with the three telescopes of the National Astronomical Observatory (NAO) Rozhen in 2011. The CCD photometric observations by using standard Bessell $BVRI$ filters cover totally 43 nights. Most of them (34 nights) were made by the 60-cm Cassegrain telescope using the FLI PL09000 CCD camera (3056 $\times$ 3056 pixels, 12 μm/pixel, field of 27.0 $\times$ 27.0 arcmin with focal reducer). The observations with the 50/70-cm Schmidt telescope equipped with the CCD camera FLI PL16803 (4096 $\times$ 4096 pixels, 9 μm/pixel, field of 1.2 $\times$ 1.2 degree) cover 12 nights. SN2011dh was observed simultaneously by the two telescopes in three nights.

The standard IDL procedures (adapted from DAOPHOT) were used for reduction of the photometric data. The transition from instrumental system to standard photometric system is made by the standard stars 2, 4, 6, 9, and 10 used by Pastorello et al. (2009) for SN2005cs. Table 1 contains the Rozhen photometric data. Each point is an average value of 3 – 4 photometric observations per night. All data are corrected for interstellar absorption and reddening appropriate to the SN2011dh direction (data from NASA/IPAC Extra-galactic Database[3] and Schlafly & Finkbeiner 2011).

[3] http://ned.ipac.caltech.edu/

Six low-dispersion spectra of the target were obtained in August and September 2011 by the 2-m RCC telescope equipped with the CCD camera VersArray 512 (512 × 512 pixels, 24 μm/pixel) and focal reducer FoReRo-2 using a grism with 300 lines/mm. The spectral resolution of these spectra was about 10.4 Å(FWHM of two pixels) and they cover the range 5100 – 7700 Å. The spectra were heliocentric corrected and shifted to the rest frame of M51 using 465 km/s (Falco et al. 1999).

3. Analysis of the observations

3.1. Photometric data

In order to obtain precise parameters describing the light curve morphology we added to our *BVRI* data those of Tsvetkov et al. (2012), Arcavi et al. (2011b), Vinko et al. (2012), and Marion et al. (2013). To unify the data we reduced additionally the observations of Tsvetkov et al. (2012), Arcavi et al. (2011b), and Vinko et al. (2012) for interstellar extinction according to the procedure used by Marion et al. (2013). Figure 1 presents the composite *BVRI* light curves of SN2011dh. They are of SN II-L type and consist of rapid decline after the light maximum and the late much slower decline.

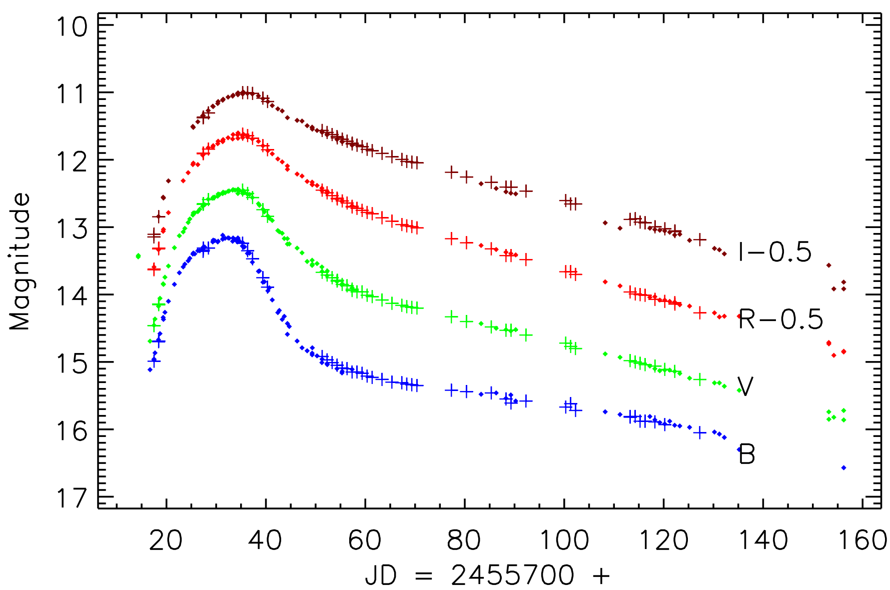

Fig. 1. Composite light curve of SN2011dh: crosses present our observations; points show all previous published observations (see the text). The vertical shifts of the R and I light curves are made for a better visibility.

Table 1. Rozhen photometry of SN2011dh

Julian Day	B [mag]	err_B [mag]	V [mag]	err_V [mag]	R [mag]	err_R [mag]	I [mag]	err_I [mag]	Telescope
2455717.488	14.970	0.011	14.461	0.019	14.132	0.003	14.146	0.010	60-cm
2455717.508	14.990	0.029	14.461	0.004	14.122	0.006	14.106	0.011	60-cm
2455718.433	14.700	0.008	14.141	0.006	13.822	0.009	13.846	0.004	60-cm
2455718.450	14.690	0.025	14.151	0.008	13.812	0.003	-	-	60-cm
2455727.380	13.360	0.017	12.661	0.021	12.402	0.005	12.376	0.003	60-cm
2455727.403	13.340	0.030	12.661	0.008	12.412	0.010	12.376	0.009	60-cm
2455727.420	13.310	0.015	12.651	0.011	12.402	0.009	12.366	0.005	50/70-cm
2455728.450	13.310	0.008	12.591	0.007	12.342	0.011	12.306	0.002	50/70-cm
2455735.325	13.240	0.030	12.451	0.017	12.122	0.006	12.006	0.009	60-cm
2455736.320	13.350	0.011	12.501	0.005	12.142	0.002	12.006	0.008	60-cm
2455737.320	13.470	0.011	12.561	0.004	12.182	0.002	12.016	0.004	60-cm
2455739.388	13.750	0.013	12.741	0.015	12.292	0.003	12.086	0.003	60-cm
2455740.333	13.890	0.006	12.841	0.004	12.352	0.002	12.136	0.002	60-cm
2455751.320	14.920	0.015	13.671	0.009	12.952	0.003	12.566	0.006	60-cm
2455752.320	14.970	0.016	13.711	0.009	12.992	0.004	12.596	0.005	60-cm
2455753.320	15.010	0.019	13.751	0.006	13.032	0.002	12.626	0.003	60-cm
2455754.320	15.050	0.017	13.801	0.006	13.072	0.006	12.656	0.009	60-cm
2455754.353	-	-	13.791	0.009	13.082	0.005	12.676	0.014	50/70-cm
2455754.350	-	-	13.791	0.012	-	-	-	-	50/70-cm
2455755.345	15.090	0.005	13.851	0.010	13.112	0.006	12.696	0.006	60-cm
2455756.335	15.100	0.020	13.871	0.013	13.142	0.012	12.726	0.004	60-cm
2455757.345	15.150	0.026	13.941	0.027	13.202	0.009	12.766	0.002	60-cm
2455757.353	-	-	13.921	0.023	13.192	0.012	12.756	0.004	50/70-cm
2455758.323	15.150	0.011	13.961	0.008	13.222	0.006	12.786	0.006	60-cm
2455759.353	15.170	0.006	13.961	0.008	13.252	0.002	12.806	0.002	60-cm
2455760.360	15.210	0.010	14.011	0.009	13.282	0.002	12.846	0.002	60-cm
2455761.378	15.230	0.021	14.031	0.015	13.302	0.002	12.866	0.003	60-cm
2455763.353	15.260	0.005	14.081	0.008	13.362	0.009	12.906	0.007	60-cm
2455765.348	15.300	0.026	14.131	0.014	13.412	0.002	12.956	0.003	60-cm
2455767.335	15.310	0.025	14.161	0.004	13.462	0.003	12.996	0.002	60-cm
2455768.330	15.330	0.016	14.181	0.005	13.482	0.004	13.026	0.004	60-cm
2455769.345	15.340	0.028	14.191	0.014	13.492	0.002	13.036	0.005	60-cm
2455770.378	15.350	0.019	14.201	0.013	13.512	0.002	13.046	0.002	60-cm
2455777.305	15.420	0.032	14.331	0.006	13.672	0.005	13.186	0.005	60-cm
2455780.338	15.440	0.030	14.401	0.004	13.732	0.013	13.256	0.005	60-cm
2455785.330	15.460	0.028	14.481	0.011	13.822	0.003	13.336	0.002	60-cm
2455788.283	15.550	0.007	14.531	0.010	13.922	0.023	13.406	0.007	50/70-cm
2455789.298	15.610	0.031	14.531	0.017	13.922	0.006	13.406	0.002	60-cm
2455792.293	15.580	0.016	14.601	0.004	13.982	0.011	13.466	0.004	60-cm
2455800.300	15.670	0.025	14.721	0.013	14.162	0.015	13.606	0.016	60-cm
2455801.290	15.620	0.031	14.771	0.018	14.162	0.008	13.656	0.018	60-cm
2455802.265	15.720	0.029	14.801	0.020	14.202	0.009	13.656	0.015	60-cm
2455813.253	15.810	0.028	14.981	0.012	14.462	0.006	13.886	0.017	50/70-cm
2455813.260	15.820	0.029	-	-	-	-	-	-	50/70-cm
2455814.283	15.810	0.024	15.001	0.030	14.492	0.021	13.876	0.015	50/70-cm
2455815.255	15.880	0.023	15.021	0.011	14.502	0.006	13.926	0.012	50/70-cm
2455816.253	15.880	0.030	15.041	0.028	14.512	0.018	13.936	0.011	50/70-cm
2455816.265	15.880	0.033	-	-	-	-	13.936	0.006	50/70-cm
2455818.240	15.890	0.019	15.061	0.009	14.572	0.009	13.996	0.008	50/70-cm
2455820.233	15.930	0.029	15.111	0.006	14.602	0.004	14.026	0.010	50/70-cm
2455822.240	-	-	15.141	0.029	14.622	0.030	14.066	0.011	60-cm
2455822.260	-	-	-	-	14.642	0.013	14.056	0.008	60-cm
2455827.268	16.050	0.035	15.261	0.030	14.772	0.009	14.186	0.005	50/70-cm

Table 2 summarizes the light curve characteristics of SN2011dh: time $JD_{\rm max}$ of the maximum light at different colors; time $JD_{\rm K}$ and magnitudes $m_{\rm K}$ of the K-point (the transition between the rapid light decline after the maximum and the slower, almost linear, decline); $BVRI$ apparent magnitudes at the maximum light $m_{\rm max}$; $BVRI$ magnitudes $m_{\rm T}$ in the first "T" days after the maximum light; $BVRI$ light decreasing $\frac{\Delta m}{\Delta t}$ during the fast and slow decline. These parameters were determined by fitting the different parts of the composite light curves with polynomials.

Table 2. Light curve parameters

Parameter		B	V	R	I
JD_{max}-2455700	[days]	32.69	33.56	34.55	35.43
JD_K-2455700	[days]	49.70	51.50	54.70	54.85
m_{max}	[mag]	13.16	12.44	12.12	12.00
m_{10}	[mag]	14.25	13.15	12.62	12.37
m_K	[mag]	14.87	13.66	13.09	12.68
m_{100}	[mag]	16.12	15.39	14.91	14.33
$\frac{\Delta m}{\Delta t}(fast)$	[mag/day]	0.100	0.068	0.048	0.035
$\frac{\Delta m}{\Delta t}(slow)$	[mag/day]	0.015	0.021	0.023	0.020
M_{max}	[mag]	-16.46	-17.18	-17.50	-17.62

The analysis of all thel photometric data led to the following results.

(a) The times of the photometric maxima of SN2011dh at different bands (Table 2) revealed that they occur later (up to 3 days) for the longer wavelengths.

(b) The light decline during the fast phase is biggest in B filter and decreases to the longer wavelengths (up to 3 times in I filter)

(c) The light decline during the slow phase is the biggest in R filter and decreases to the shorter wavelengths (up to 1.5 times in B filter).

(d) The K-point is best defined in B filter and occurs around 17 days after the B light maximum.

(e) Using the recent distance value of 8.4 Mpc (Vinco et al. 2012) and the values of $m_{\rm max}$ (Table 2) we obtained the absolute magnitudes $M_{\rm max}$ of SN2011dh at different bands (last raw of Table 2). The obtained values support the conclusion that the most SNe II-L have a peak absolute magnitude around 2.5 mag fainter than SNe Ia (Young & Branch 1989, Gaskell 1992).

(f) The shapes of the color curves $B-V$ and $V-R$ (Fig. 2) are similar. They show that SN2011dh quickly reddens until the K-point, and then gradually becomes more bluer. The amplitudes of the $B-V$ and $V-R$ changes are around 0.8 mag and 0.5 mag respectively. The $R-I$ color curve has no extremum and the beginning of its slower increasing is around the time of the K-point.

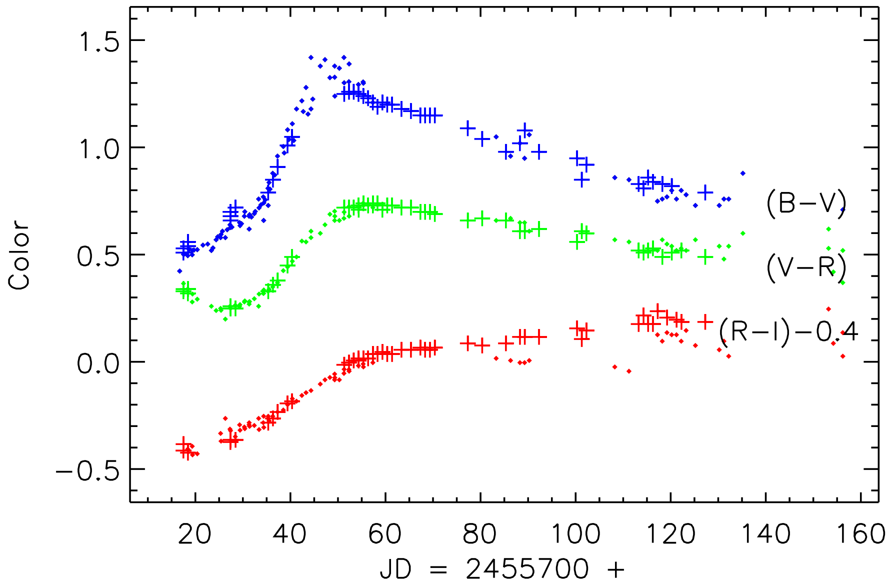

Fig. 2. $B-V$, $V-R$ and $V-I$ color curves of SN2011dh (the vertical shift of the $R-I$ curve is made for a better visibility). The symbols are the same as in Fig. 1

3.2. Low-dispersion spectra

The low-resolution spectra of SN2011dh from August and September 2011 (2-3 months after the light maximum) exhibit very broad (FWHM around 100 Å) spectral features making the continuum identification quite difficult (Fig. 3). The broad lines are indication for the large ranges of the expansion velocities, typical for SN II type.

The Hα line is visible as a weak absorption feature in the first 2 spectra from the beginning of August 2011 (Fig. 3). The earlier spectral history of SN 2011dh (Vinko et al. 2012, Marion et al. 2013) revealed rapidly weakening of the Hα line as well as its transformation from an emission feature with a P-Cygni profile to a symmetric absorption at the beginning of July 2011. Our spectra from the beginning of August 2011 show that the Hα line has continued to weaken and its profile has become asymmetric but with higher left shoulder (see for comparison figs. 5 and 8 in Marion et al. 2013). The weakening of the Hα feature reached to its gradual disappearing in the last four spectra taken 3–4 weeks later (Fig. 3).

The most prominent absorption feature of all Rozhen spectra is that at 5745 Å associated with HeI 5876 (contaminated by NaI D). This feature appeared 11 days after the explosion, became progressively stronger and almost equaled the Hα feature in depth and width at the end of June (Vinko et al. 2012, Marion et al. 2013). At the beginning of August the HeI 5876 feature turned out even considerably (4-5 times) deeper and broader than the Hα line (Fig. 3).

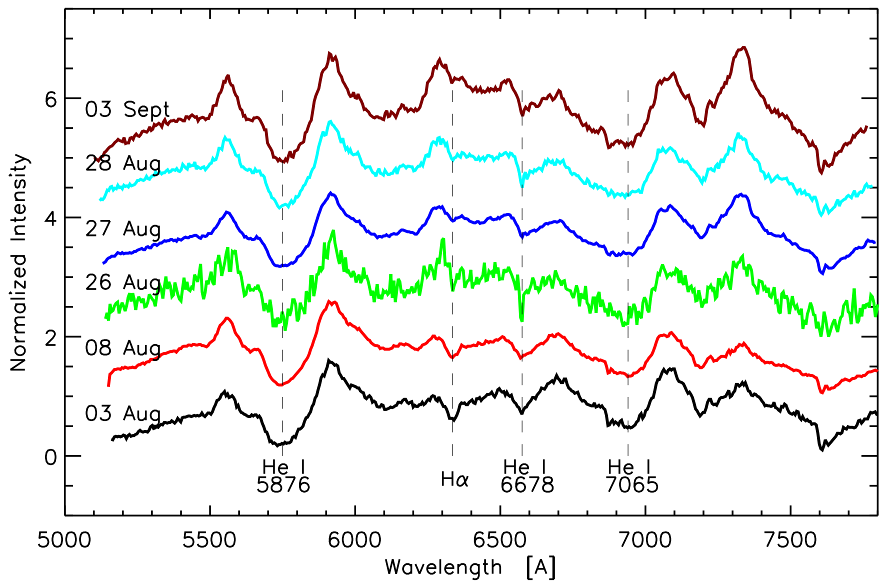

Fig. 3. The spectra of SN2011dh obtained at NAO Rozhen

The Rozhen spectra exhibited prominent features HeI 6678 and HeI 7065 which strengthened simultaneously with HeI 5876. They were scarcely visible in the spectra of SN2011dh taken a month earlier (Marion et al. 2013).

Thus, our spectra present continuation of the spectral history of SN2011dh. The disappearing of the Hα line as well as the strengthening of the HeI features around three months after the light maximum provide additional, sure confirmations that the Supernova SN2011dh is a new member of the rare SN IIb family.

In fact, Arcavi et al. (2011b) made the first supposition about the IIb subtype of SN2011dh without identifying He features, only due to its similarity with SN1993J. They noted that its spectra were dominated by H lines out to day 10 after explosion, but initial signs of He appeared to be present. Arcavi et al. (2011b) assumed that if the He lines continue to develop in the near future, then SN2011dh would turn out a member of the cIIb class. Marion et al. (2011) confirmed the type IIb classification with the first detection of HeI lines in NIR spectra obtained 16 days after the explosion. Maund et al. (2011) identified HeI lines in optical spectra and found that the transition from H dominated spectra to He is nearly complete 40 days after the explosion. The spectra of Vinko et al. (2012) and Marion et al. (2013) exhibit the presence of optical HeI features 12 days after the explosion. The spectra taken at NAO Rozhen around 2.5 – 3 months after the explosion gave the next arguments about the IIb classification of SN2011dh.

In order to determine the quantitative characteristics (velocities, widths, etc.) we fitted the spectral lines with polynomials.

The Doppler shifts of the Hα line of our spectra in August 2011 correspond to mean expansion velocity of 9880 km/s (Table 3). This value is by 1920 km/s smaller than that of the last spectrum of Marion et al. (2013) from the beginning of July. In fact, the Hα velocities declined rapidly from 15400 km/s to about 12500 km/s in the first 2 weeks after the explosion (Marion et al. 2013) and then continued gradually to decrease.

The Doppler shifts of the HeI 5876 feature of the Rozhen spectra correspond to mean velocity of 6240 km/s. This value is by 1560 km/s smaller than that of the last spectrum from the beginning of July (Marion et al. 2013).

The difference between the expansion velocities of Hα and HeI 5876 in August was around 3640 km/s. This difference has been 4000 km/s at the beginning of July (Table 3). Thus, our results confirmed the trend the hydrogen line-forming region to be considerably separated from the helium layer (Marion et al. 2013).

The Doppler shifts of HeI 6678 and HeI 7065 of our spectra correspond to mean expansion velocities of 4160 km/s and 5250 km/s (Table 3). These values are considerably smaller than that of HeI 5876. Moreover, the biggest decreasing of the expansion velocity from the beginning of July of is that of HeI 6678.

The different velocities of the observed spectral features of HI and HeI correspond to the different physical conditions (temperature, pressure, opacity, etc.) and chemical composition of outer layers of the exploded star with an "onion" structure.

Table 3. Velocity measurements of Hα and HeI lines (in units km/s)

Date	Hα	HeI 5876	HeI 6678	HeI 7065
Jul 04.2*	11800	7800	7100	6800
Aug 03.82	9850	6100	4200	4700
Aug 08.82	9850	6450	4400	4600
Aug 26.78	9850	6400	4100	5300
Aug 27.78	9850	6400	3950	5650
Aug 28.78	9850	6100	4150	6000
Sept 03.78	10000	6000	4150	5250

*The last spectrum of Marion et al. (2013)

Conclusion

The results from this study allow us to infer the following conclusions.

1. The light curve of SN2011dh is of SN II-L type with a peak absolute magnitude of $M_V = -17.18^m$. The light maxima occur later (up to 3 days) for the longer wavelengths.
2. The light decline during the fast phase is the biggest in B and decreases to the longer wavelengths (up to 3 times in I band) while the light decline during the slow phase is the biggest in R and decreases to the shorter wavelengths (up to 1.5 times in B band).

3. The HeI 5876 feature at the beginning of August 2011 was considerably (4 – 5 times) deeper and broader than the Hα line while they were almost the same a month earlier.
4. The expansion velocity of the Hα line at the beginning of August 2011 is around 9880 km/s and nearly 1920 km/s smaller than that a month earlier.
5. The expansion velocity of the HeI 5876 feature is around 6240 km/s, i.e. by 3640 km/s smaller than that of the Hα line.
6. The disappearing of the Hα line and the strengthening of the HeI features at the end of August 2011 provided additional confirmations that the Supernova SN2011dh is a new member of the rare SN IIb family.

The SNe phenomena of subtype IIb are poorly studied due to their rareness. SN1987K was the first representative with such strange spectral behavior (Fillipenko 1988) but SN 1993J best defined the optical properties of a SN IIb. Recently, Chevalier & Soderberg (2010) included additional (non-optical) distinguishing features of the SN IIb subtype: rapidly evolving radio emission, rapid expansion of the radio shell, nonthermal X-ray emission. Several SNe have one or more of these features: 1996cb, 2001ig, 2003bg, 2008ax, 2008bo, and 2001gd.

The explosion of the very nearby SN20111dh offered the unique opportunity to study the evolution of an exceptionally rare event of IIb subtype.

The observations obtained at NAO Rozhen provided continuation of the spectral history of SN2011dh during the third month after the explosion tracking the gradual transition from HI dominated spectra to HeI ones. These empirical data can be used as constraints for the SN IIb models and for explanation of the mechanism responsible for the removal of the outer envelope before the explosion.

Our results could be considered as some contribution in the study of the rare SN IIb phenomena exhibiting the explosive end of massive stars which H envelope is kept before the explosion. Recently they become still more interesting due to the detection of their connection with the long-duration gamma-ray bursts (Woosley & Bloom 2006).

Acknowledgements

This research has made use of the NASA/IPAC Extragalactic Database (NED) which is operated by the Jet Propulsion Laboratory, California Institute of Technology, under contract with the National Aeronautics and Space Administration. The study was supported by funds of the projects DO 02-362, DO 02-85, and DDVU 02/40-2010 of the Bulgarian National Science Fund as well as the project RD 08-261 of Shumen University.

References

Arcavi I. et al., 2011a, ATel 3413
Arcavi I. et al., 2011b, ApJ 742L, 18
Benvenuto O., Bersten M., Nomoto K., 2013, ApJ 762, 74
Bersten M., Benvenuto O., Nomoto K., 2012, IAUS 279, 18
Chevalier R., Soderberg A., 2010, ApJ 711, L40
Ensman L., Woosley S.E., 1987, BAAS 19, 1036
Ergon M. et al., 2013, ATel 4912
Falco E. et al., 1999, PASP 111, 438
Fillipenko A., 1988, AJ 96, 1941
Fillipenko A., 1993, AAS 182, 1902
Fillipenko A., 1997, ARA&A 35, 309
Gaskell C., 1992, ApJ 389L, 17
Georgy C., 2012, A&A 538L, 8
Horesh A. et al., 2011a, ATel 3411
Horesh A. et al., 2011b, ATel 3405
Kasliwal M. et al., 2011, ATel 3402
Law N.M., Kulkarni S.R., Dekany R.G., Ofek E.O., et al., 2011, PASP 121, 1395
Margutti R., Soderberg A., 2011, ATel 3400, 1
Marion G. et al., 2011, ATel. 3435
Marion G. et al., 2013, arXiv:1303.5482v1
Marti-Vidal I. et al., 2011 A&A 535L, 10
Maund J. et al., 2011 ApJ 739L, 37
Nomoto K., Suzuki T., Shigeyama T., Kumagai S., 1993, AAS 183, 3904
Pastorello A. et al., 2009, MNRAS 394, 2266
Riou, A. et al., 2011, CBET 2736
Schlafly E., Finkbeiner D., 2011, ApJ 737, 103
Silverman J. et al., 2011, ATel 3398
Soderberg A., Margutti R., Zauderer B., Krauss M. et al., 2012, ApJ 752, 78
Szczygie D., Gerke J., Kochanek C., Stanek K., 2012, ApJ 747, 23
Tsvetkov D. et al., 2012, PZ 32, 6
Van Dyk S. et al., 2011, ApJ 741L, 28
Van Dyk S. et al., 2013, ATel 4850
Vinko J. et al., 2012, A&A 540A, 93
Woosley S., Eastman R., Weaver T., Pinto P., 1994, ApJ 429, 300
Woosley S. E., Bloom J. S., 2006, ARA&A 44, 507
Young T., Branch D., 1989, ApJ 342L, 79